# *Thermophysical Properties of Cold- and Vacuum Plasma-Sprayed Cu-Cr-X Alloys, NiAl and NiCrAlY Coatings II: Specific Heat Capacity*

**S. V. Raj**

**Journal of Materials Engineering and Performance**

ISSN 1059-9495

J. of Materi Eng and Perform
DOI 10.1007/s11665-017-3015-x

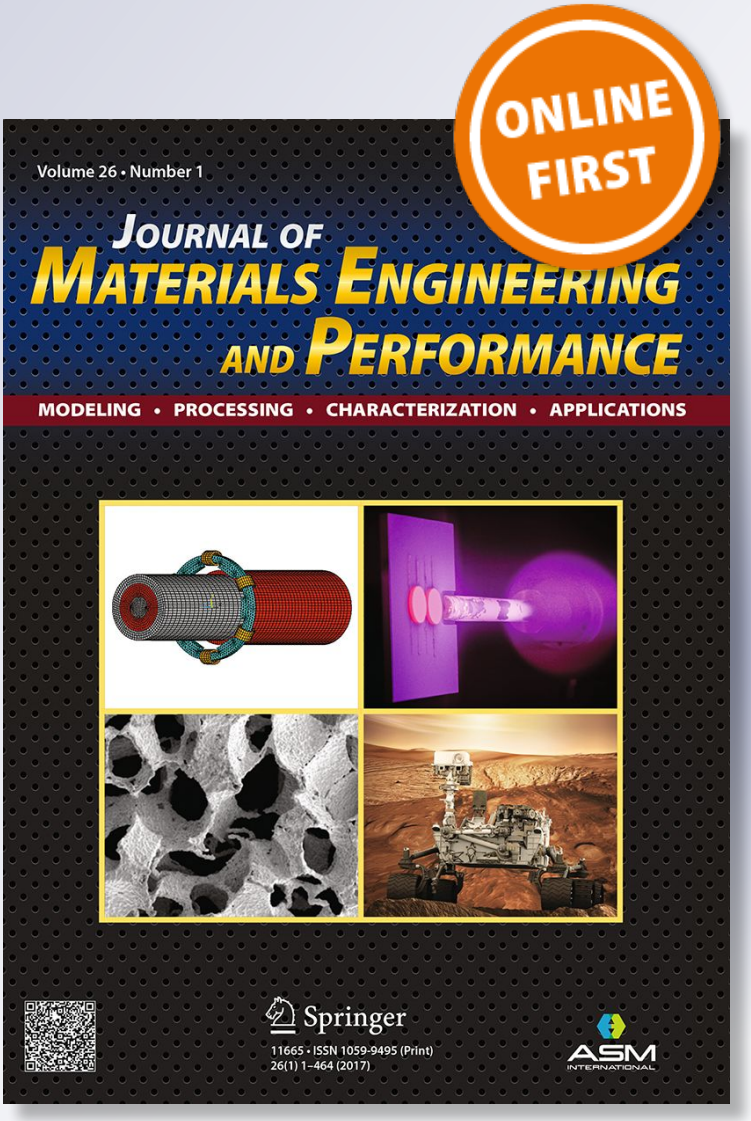


Springer

JMEPEG
DOI: 10.1007/s11665-017-3015-x


1059-9495/$19.00

# Thermophysical Properties of Cold- and Vacuum Plasma-Sprayed Cu-Cr-X Alloys, NiAl and NiCrAlY Coatings II: Specific Heat Capacity

*S.V. Raj*

*(Submitted September 8, 2017)*

**Part I of the paper discussed the temperature dependencies of the electrical resistivities, thermal conductivities, thermal diffusivities and total hemispherical emissivities of several vacuum plasma-sprayed (VPS) and cold-sprayed (CS) copper alloy monolithic coatings, VPS NiAl, VPS NiCrAlY, extruded GRCop-84 and as-cast Cu-17(wt.%)Cr-5%Al. Part II discusses the temperature dependencies of the constant-pressure specific heat capacities, $C_P$, of these coatings. The data were empirically regression-fitted with the equation:**

$$C_P = AT^4 + BT^3 + CT^2 + DT + E$$

**where $T$ is the absolute temperature and $A$, $B$, $C$, $D$ and $E$ are regression constants. The temperature dependencies of the molar enthalpy, molar entropy and Gibbs molar free energy determined from experimental values of molar specific heat capacity are reported. Calculated values of $C_P$ using the Neumann–Kopp (NK) rule were in poor agreement with experimental data. Instead, a modification of the NK rule was found to predict values closer to the experimental data with an absolute deviation less than 6.5%. The specific molar heat capacities for all the alloys did not agree with the Dulong–Petit law, and $C_P > 3R$, where $R$ is the universal gas constant, were measured for all the alloys except NiAl for which $C_P < 3R$ at all temperatures.**

**Keywords** aerospace, cold- and vacuum plasma-sprayed coatings, copper alloys, Neumann–Kopp rule, NiAl and NiCrAlY, specific heat capacity, thermodynamic functions

## 1. Introduction

As noted in Part I (Ref 1), an evaluation of the thermophysical properties of materials is important both for gaining a fundamental understanding of material behavior, as well as in engineering applications, such as structural design of components and systems. Environmental and thermal barrier protective metallic coatings designed for aerospace applications, such as reusable launch vehicle (RLV) combustion liners, turbine blades and vanes, are commonly deposited by conventional cold and vacuum plasma spray processes. The deposition of these coatings on the substrates results in the development of residual stresses which can affect the performance and durability of the coating-substrate system. In the case of aerospace applications, modeling the heat transfer behavior and stress analyses of the coating-substrate system is crucial for predicting component performance and life. Part 1 discussed the microstructures, densities and temperature dependencies of electrical resistivity, thermal conductivity, thermal diffusivity and total hemispherical emissivity of several vacuum plasma-sprayed (VPS) and cold-sprayed (CS) copper alloy monolithic coatings, VPS NiAl, VPS NiCrAlY, extruded GRCop-84 and as-cast Cu-17(wt.%)Cr-5%Al. The objective of Part II is to report the constant-pressure specific heat capacities, $C_P$, of these materials as a function of absolute temperature, $T$.

## 2. Experimental Procedures

The nominal compositions of the alloy powders investigated in this research were Cu-8(wt.%)Cr, Cu-26(wt.%)Cr, Cu-8(wt.%)Cr-1%Al, Cu-23(wt.%)Cr-5%Al, Ni-31.5(wt.%)Al (NiAl), Ni-17(wt.%)Cr-6%Al-0.5%Y (NiCrAlY). Monolithic coatings* were sprayed on mandrels either by cold or vacuum plasma spray methods. Details of the powder suppliers and fabrication methods were reported earlier (Ref 2-4) and summarized in Part I (Ref 1). In addition, extruded GRCop-84 and an as-cast Cu-17(wt.%)Cr-5%Al alloy were also investigated. The batch I.D.s used in this paper are given in Table 2 in Part I (Ref 1).

As noted in Part I (Ref 1), the thermophysical property measurements reported in Parts I and II were conducted at Thermophysical Properties Research Laboratory, Inc. (TPRL), West Lafayette, IN under contract. Constant-pressure specific heat was measured between 295 and 1223 K using a standard Perkin–Elmer model DSC-2 differential scanning calorimeter using sapphire as the reference material in accordance with ASTM E1269 (Ref 5, 6), where the sapphire and the experimental specimens were subjected to an identical heat

**S.V. Raj,** NASA Glenn Research Center, MS 106-5, 21000 Brookpark Road, Cleveland, OH 44135. Contact e-mail: sai.v.raj@nasa.gov.

*The term "monolithic coatings" is used in a generic manner in this paper to distinguish cold- and vacuum plasma-sprayed powders from cast or extruded alloys.



Published online: 23 October 2017

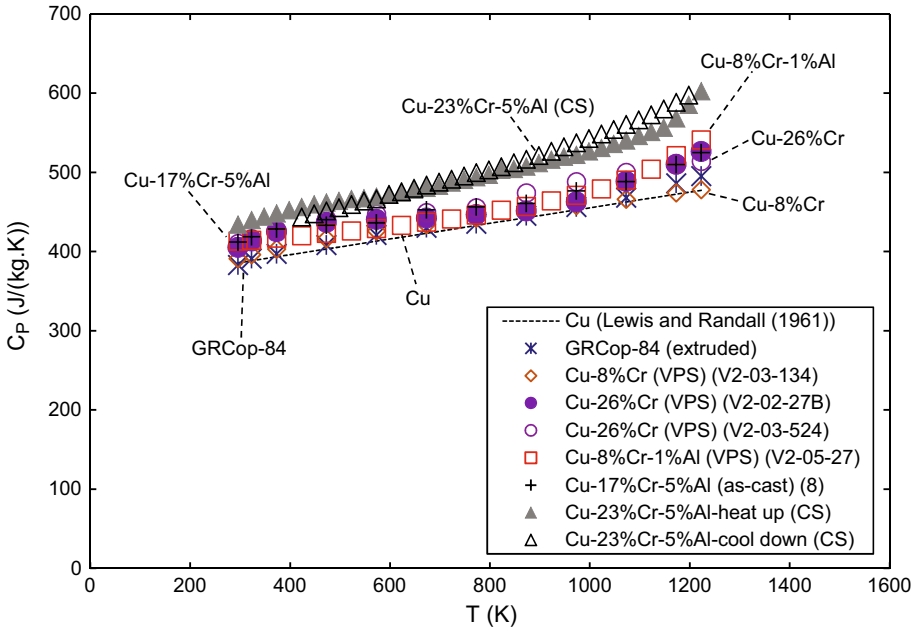


**Fig. 1** Temperature dependencies of the specific heat capacities for extruded GRCop-84, and VPS Cu-8%Cr, VPS Cu-26%Cr (V2-03-524), VPS Cu-8%Cr-1%Al, as-cast Cu-17%Cr-5%Al, and CS Cu-23%Cr-5%Al

flux. The differential powers required to heat both the reference and the experimental specimens at identical rates were recorded by a computerized data acquisition system. The specific heat of the experimental specimen was calculated from the known specific heat of sapphire, masses of the sapphire standard and specimen, and the differential power.

## 3. Results and Discussion

### 3.1 Constant-Pressure Specific Heat Capacities of Copper Alloys

Figure 1 shows the variations of the experimental values of $C_P$ with $T$ for extruded GRCop-84, VPS Cu-8%Cr, VPS Cu-26%Cr, VPS Cu-8%Cr-1%Al, as-cast Cu-17%Cr-5%Al and CS Cu-23%Cr-5%Al. The broken line represents the magnitudes of $C_P$ for Cu calculated from the equation published by Lewis and Randall (Ref 7). In all cases, the magnitudes of $C_P$ increase with increasing values of absolute temperature. An examination of Fig. 1 reveals that the data fall into two categories. First, the values of $C_P$ for all the alloys except CS Cu-23%Cr-5%Al are clustered in a narrow range close to those for copper (Ref 7) with the maximum deviation of about 13.5% for Cu-8%Cr-1%Al occurring at 1223 K. Thus, $(C_P)_{Cu} \sim 386$ J/kg K at 295 K for Cu and $(C_P)_{Cu} \sim 477$ J/kg K at 1223 K (Ref 7). In comparison, $(C_P)_{Cu8Cr1Al} \sim 413$ J/kg K at 295 K increasing to $(C_P)_{Cu8Cr1Al} \sim 541$ J/kg K at 1223 K. Second, the magnitudes of $C_P$ for CS Cu-23%Cr-5%Al coating exhibit an increasing deviation from the clustered data for the other alloys with increasing temperature. In this case, $(C_P)_{Cu23Cr5Al} \sim 434$ J/kg K at 295 K and $(C_P)_{Cu8Cr1Al} \sim 602$ J/kg K at 1223 K.

A fourth-order NASA polynomial equation** given by Eq 1 was used to regression fit the data shown in Fig. 1 (Ref 8-10).

$$C_P = A * T^4 + B * T^3 + C * T^2 + D * T + E(\text{J/kg K}) \quad \text{(Eq 1)}$$

where $A$, $B$, $C$, $D$ and $E$ are the regression constants. Table 1 gives the magnitudes of these coefficients for the copper alloys shown in Fig. 1 as well as the corresponding coefficients of determination, $R_d^2$ for each material. It was confirmed that the regressed values and the experimental data were in excellent agreement for all the alloys.

Figure 2 compares the temperature dependencies of $C_P$ for VPS GRCop-84 (Ref 11) with those for extruded GRCop-84 reported in the present paper. The two sets of data are in excellent agreement irrespective of the processing method.

### 3.2 Constant-Pressure Specific Heat Capacities of Nickel Alloys

Figure 3 shows the variation of $C_P$ with $T$ for VPS NiAl and the two batches of VPS NiCrAlY. The literature data for Ni (Ref 12) and stoichiometric NiAl single crystal (Ref 13) are also included. As shown in Fig. 3, the data for single-crystal NiAl (Ref 13) and polycrystalline VPS NiAl are in excellent agreement increasing from 550 J/kg K at 295 K to 650 J/kg K at 1223 K. This suggests that $C_P$ is insensitive to processing method, grain size and crystal orientation in stoichiometric NiAl. The values of $C_P$ for NiAl are higher than those for VPS NiCrAlY below 973 K, and at nearly all temperatures, for Ni (Ref 12). The $C_P$ data for both batches of VPS NiCrAlY are almost identical at and below 973 K, but the two sets of deviate above 973 K with the values for $C_P$ increase significantly with increasing absolute temperature for the denser batch of NiCrAlY (V2-03-528). The values of $C_P$ are also higher than those for NiAl above 973 K. Overall, the magnitudes of $C_P$ for NiCrAlY (V2-03-528) increase from 455 J/kg K at 295 K to 789 J/kg K at 1223 K. The regression coefficients were

**It is noted that the NASA polynomial equation was a better fit to the experimental data than the other commonly used empirical equation $C_P = E_1 + D_1 * T + C_1/T^2$ [7].

**Table 1 Regression coefficients determined by fitting Eq 1 to the experimental data shown in Fig. 1 and 2, and the corresponding values of $R_d^2$**

| Material | *A*, J/kg K$^5$ | *B*, J/kg K$^4$ | *C*, J/kg K$^3$ | *D*, J/kg K$^2$ | *E*, J/kg K | $R_d^2$ |
|---|---|---|---|---|---|---|
| GRCop-84 (Extruded) | $-1.8 \times 10^{-11}$ | $2.4 \times 10^{-7}$ | $-4.6 \times 10^{-4}$ | 0.39 | 302.0 | 0.9989 |
| Cu-8%Cr (V2-03-134) | $-1.2 \times 10^{-10}$ | $4.4 \times 10^{-7}$ | $-5.9 \times 10^{-4}$ | 0.42 | 306.8 | 1.0000 |
| Cu-26%Cr (V2-02-27B) | $-5.4 \times 10^{-10}$ | $2.1 \times 10^{-6}$ | $-2.6 \times 10^{-3}$ | 1.40 | 171.8 | 0.9986 |
| Cu-26%Cr (V2-03-524) | $-9.3 \times 10^{-10}$ | $2.9 \times 10^{-6}$ | $-3.2 \times 10^{-3}$ | 1.50 | 167.0 | 0.9970 |
| Cu-8%Cr-1%Al (V2-05-27) | $3.3 \times 10^{-10}$ | $-7.8 \times 10^{-7}$ | $7.2 \times 10^{-4}$ | −0.23 | 436.1 | 0.9997 |
| Cu-17%Cr-5%Al (as-cast) (8) | $5.6 \times 10^{-11}$ | $5.8 \times 10^{-8}$ | $-2.7 \times 10^{-4}$ | 0.28 | 354.0 | 0.9936 |
| Cu-23%Cr-5%Al-heat up (CS) | $4.0 \times 10^{-10}$ | $-9.4 \times 10^{-7}$ | $7.8 \times 10^{-4}$ | −0.15 | 435.4 | 0.9949 |
| Cu-23%Cr-5%Al-cool down (CS) | $9.0 \times 10^{-11}$ | $-1.2 \times 10^{-7}$ | $1.9 \times 10^{-5}$ | 0.19 | 366.8 | 0.9999 |
| NiAl (V2-03-166) | $-3.1 \times 10^{-11}$ | $1.4 \times 10^{-7}$ | $-2.9 \times 10^{-4}$ | 0.36 | 466.3 | 0.9998 |
| Ni-17%Cr-6%Al-0.5%Y (V2-02-27E) | $-1.3 \times 10^{-9}$ | $4.1 \times 10^{-6}$ | $-4.4 \times 10^{-3}$ | 2.10 | 140.1 | 0.9964 |
| Ni-17%Cr-6%Al-0.5%Y (V2-03-528) | $-1.2 \times 10^{-9}$ | $4.3 \times 10^{-6}$ | $-5.2 \times 10^{-3}$ | 2.60 | 313.4 | 0.9999 |

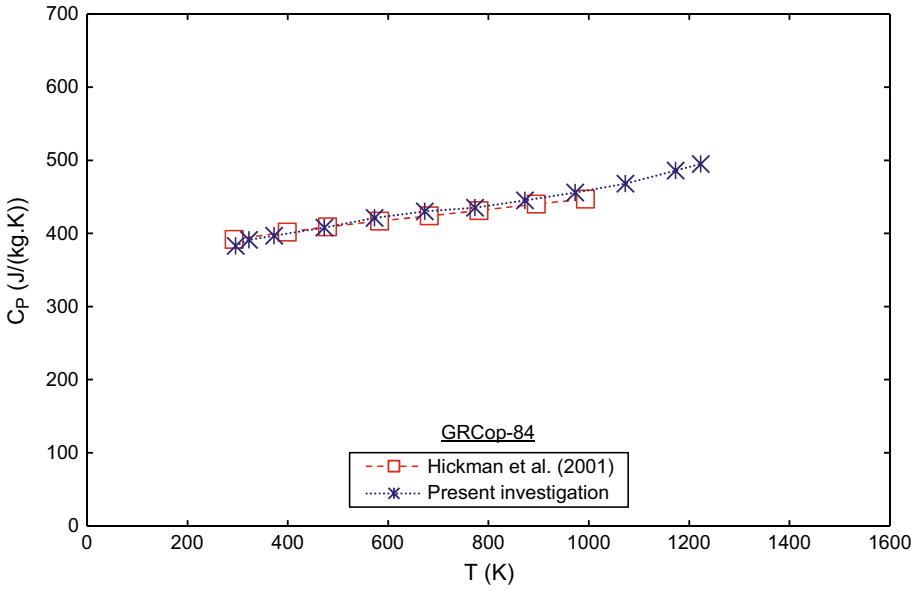


**Fig. 2** Comparison of the temperature dependencies of the specific heat capacities for extruded GRCop-84 determined in the present investigation with those reported for VPS GRCop-84 (Ref 8)

determined by fitting Eq 1 to the data for VPS NiAl and VPS NiCrAlY, and the values of these coefficients and their corresponding $R_d^2$ are given in Table 1. Figure 4 compares the specific heat capacities of the copper and nickel-based alloys investigated in the present investigation. The specific heat capacities of NiAl and NiCrAlY are larger than those for the copper coating alloys and GRCop-84 substrate.

### 3.3 Comparison of the Experimental Data with the Neumann–Kopp Rule

The empirical Neumann–Kopp (NK) rule is often used to estimate the heat capacities of compounds formed from their constituent elements with some degree of success although several deviations have been noted in the literature (Ref 7, 14-17). In the case of alloys formed by mixing *M* elements, the NK rule states that the specific heat capacity of the alloy, $(C_P)_{NK}$, is given by

$$(C_P)_{NK} = f_1 * C_1 + f_2 * C_2 + f_3 * C_3 + \cdots + f_N * C_M \quad \text{(Eq 2)}$$

where $f_i$ is the atom percent of the *i*th element with a specific heat capacity, $C_i$, and $i = 1,2,3,\ldots M$.

Figures 5 and 6 compare the temperature dependencies of the experimental,[†] $(C_P)_{expt}$, and predicted values using Eq 2 for the copper- and nickel-based alloys studied in the present investigation. For the copper alloys, $(C_P)_{NK} > (C_P)_{expt}$ at most temperatures, where the absolute deviations[‡] varied between 0.5 and 14% depending on absolute temperature; however, the values of $(C_P)_{NK} \sim (C_P)_{expt}$ for the Cu-23%Cr-5%Al within an absolute deviation of 5% (Fig. 5). The magnitudes of $(C_P)_{NK} \gg (C_P)_{expt}$ for NiAl and NiCrAlY with the absolute deviations varying between 18 and 44% for NiAl and 8 and 12% for NiCrAlY, respectively (Fig. 6). In contrast, Brandt et al. (Ref 18), who observed that the absolute deviations varied between 0.22 and 11.99% for a Ni-9.94(at.%) Al alloy, concluded that the agreement between the experimental and the predicted values were reasonable.

[†]Although $C_P$ was used to describe the experimental data in Fig. 1, 2, 3, and 4, the term $(C_P)_{expt}$ is used in Fig. 5, 6 and 7 specifically to distinguish the experimental data from the values calculated using Eq 2. It is noted that the experimental data shown in Fig. 5, 6 and 7 are identical to those shown in Fig. 1, 2, 3 and 4.

[‡]The deviation was defined as $((C_P)_{NK} - (C_P)_{expt})/(C_P)_{expt})$. Only absolute values are reported.

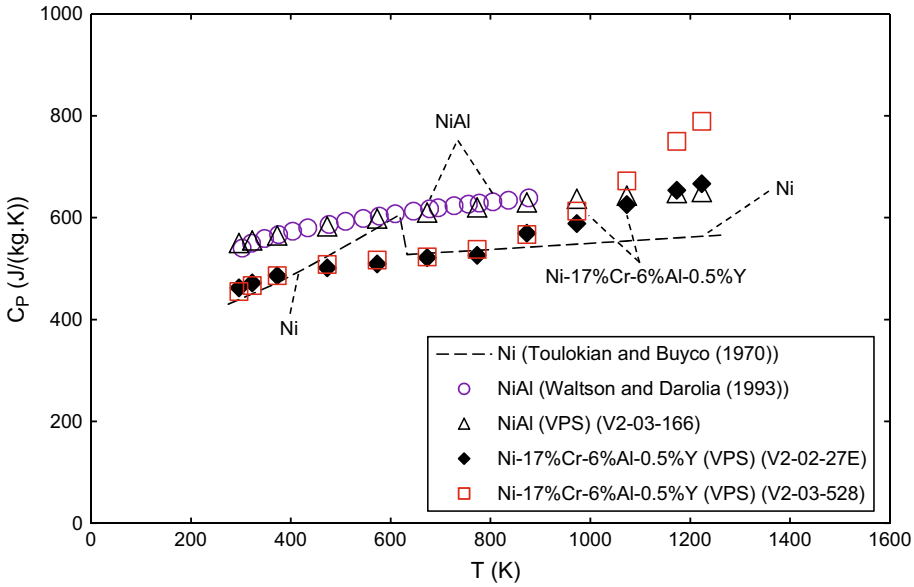


**Fig. 3** Temperature dependencies of the specific heat capacities for VPS NiAl and VPS Ni-17(wt.%)Cr-6%Al-0.5%Y. The present data are compared with literature data on Ni (Ref 9) and NiAl single crystal (Ref 10)

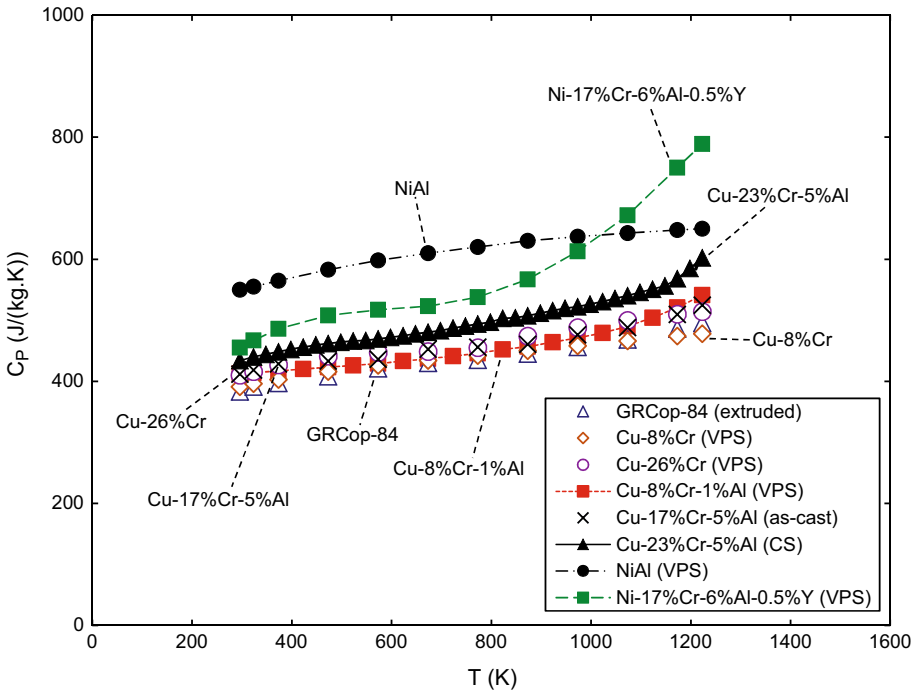


**Fig. 4** Comparison of the specific heat capacities for extruded GRCop-84, VPS Cu-8%Cr, VPS Cu-26%Cr (V2-03-524), VPS Cu-8%Cr-1%Al, as-cast Cu-17%Cr-5%Al, CS Cu-23%Cr-5%Al, VPS NiAl (V2-03-166) and Ni-17(wt.%)Cr-6%Al-0.5%Y (V2-03-528)

A plot of $(C_P)_{NK}$ against $(C_P)_{expt}$ provided additional insights into the extent of disagreement between the predicted and the experimental values (Fig. 7). It is noted that the broken line at 45° in Fig. 7 represents the case when $(C_P)_{NK} = (C_P)_{expt}$. An examination of Fig. 7 reveals that the predicted values determined from Eq 2 are generally significantly larger than the experimentally measured values of $C_P$ except in a narrow region, where the symbols are close to the 45° line. However, as noted earlier, the agreement between the experimental and the predicted values is reasonably good for the CS Cu-23%Cr-5%Al coating within 5%.

A close examination of the data shown in Fig. 7 suggests that it may be possible to fit a single curve through the data for all the materials reported in the present paper. A regression fit revealed that $(C_P)_{NK}$ and $(C_P)_{expt}$ correlate very well through Eq 3:

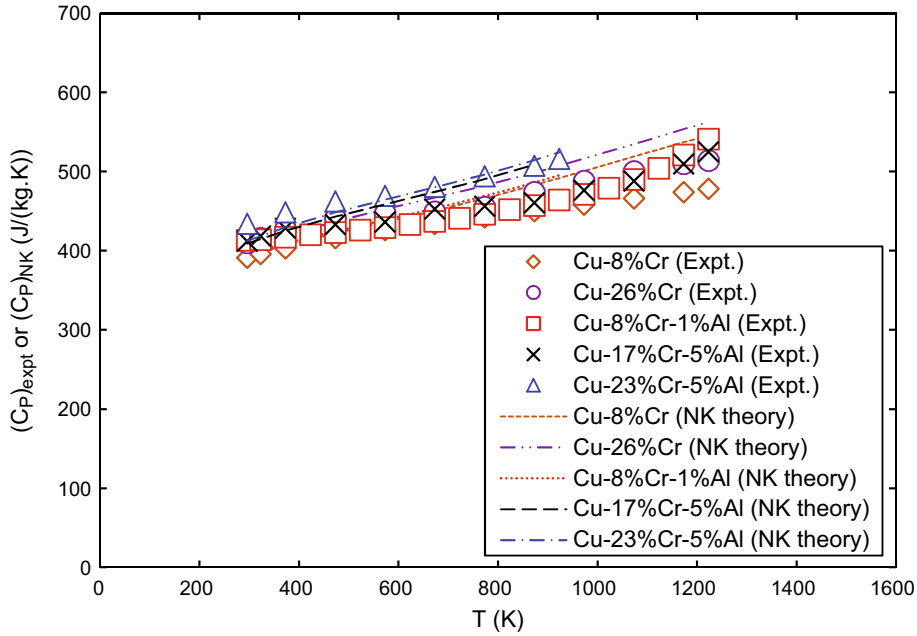


**Fig. 5** Comparison of the experimental, $(C_P)_{expt}$, and calculated Neumann–Kopp, $(C_P)_{NK}$, specific heat capacities for extruded GRCop-84, and VPS Cu-8%Cr, VPS Cu-26%Cr (V2-03-524), VPS Cu-8%Cr-1%Al, as-cast Cu-17%Cr-5%Al, and CS Cu-23%Cr-5%Al

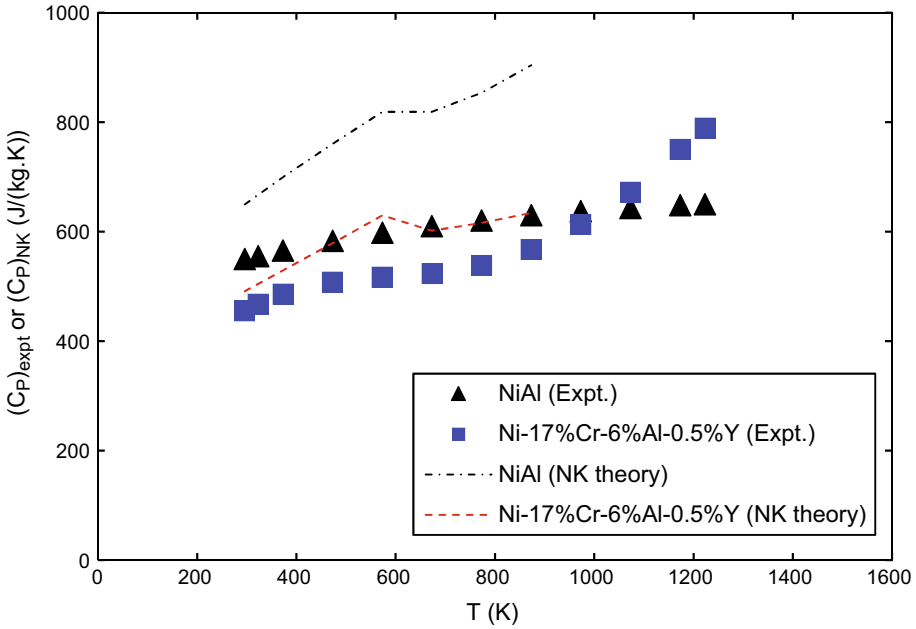


**Fig. 6** Comparison of the experimental and calculated Neumann–Kopp specific heat capacities for VPS NiAl and VPS Ni-17(wt.%)Cr-6%Al-0.5%Y (V2-03-528)

$$(C_P)_{NK} = 98.505 * \exp\left[-0.0035 * (C_P)_{expt}\right] \text{ (J/kg K)} \quad \text{(Eq 3)}$$

with a $R_d^2 = 0.9516$. Rearranging the terms in Eq 3, the magnitudes of $C_P$ for an alloy or a compound with i elements with known values of $C_i$, where $(C_P)_{NK}$ is calculated from Eq 2, can be estimated from

$$C_P = 288.68 * \ln\left(\frac{98.505}{(C_P)_{NK}}\right) \text{ (J/kg K)} \quad \text{(Eq 4)}$$

The absolute deviation, $|\Delta|$, between the values estimated from Eq 4 and the experimental measurements of $C_P$ for the materials shown in Fig. 7 varied between 0.1 and 6.5%. Despite this excellent agreement, it is cautioned that the general validity of Eq 4 for estimating the magnitudes of $C_P$ for other materials needs to be proven.

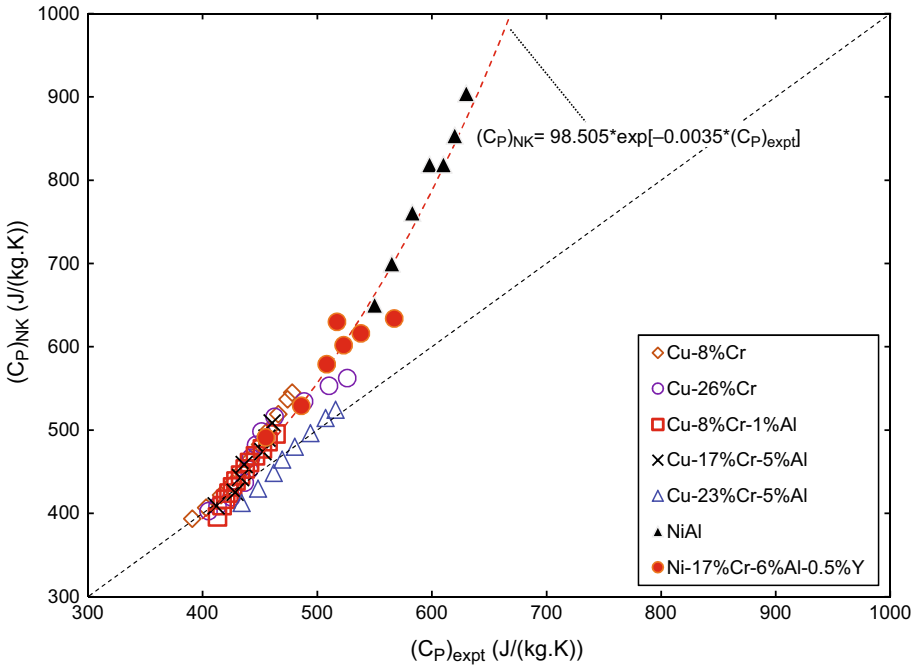


**Fig. 7** Plot of the calculated Neumann–Kopp specific heat capacity against the experimental specific heat capacity showing the extent of deviation from the 45° line for the different alloys

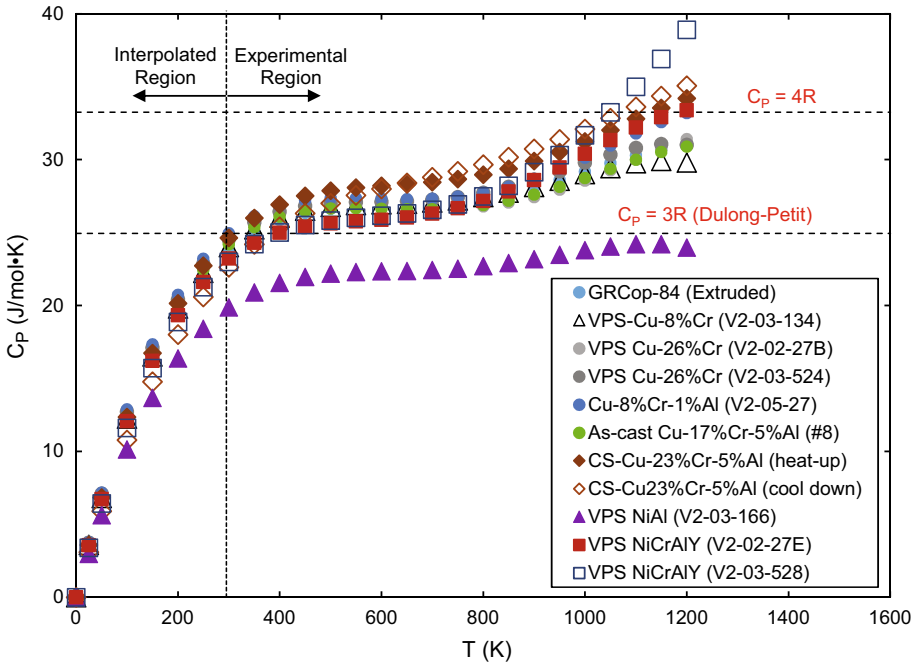


**Fig. 8** Plot of the specific molar heat capacity against the absolute temperature for the copper alloys, NiAl and NiCrAlY alloys. The experimental data lie to the right of the vertical broken line, while the symbols to the left of this line are interpolations of the regression equations to the experimental data. The two horizontal broken lines represent values of $C_P = 3R$ or $4R$

**Table 2 Regression coefficients determined by fitting Eq 3 to the experimental data shown in Fig. 1 and 2, and the corresponding values of $R_d^2$**

| Material | $A$, J/mol K$^5$ | $B$, J/mol K$^4$ | $C$, J/mol K$^3$ | $D$, J/mol K$^2$ | $R_d^2$ |
|---|---|---|---|---|---|
| GRCop-84 (Extruded) | $-8.1 \times 10^{-11}$ | $2.6 \times 10^{-7}$ | $-3.0 \times 10^{-4}$ | 0.15 | 0.9998 |
| Cu-8%Cr (V2-03-134) | $-8.8 \times 10^{-11}$ | $2.8 \times 10^{-7}$ | $-3.1 \times 10^{-4}$ | 0.15 | 0.9998 |
| Cu-26%Cr (V2-02-27B) | $-7.6 \times 10^{-11}$ | $2.6 \times 10^{-7}$ | $-3.1 \times 10^{-4}$ | 0.15 | 0.9999 |
| Cu-26%Cr (V2-03-524) | $-9.8 \times 10^{-11}$ | $3.1 \times 10^{-7}$ | $-3.4 \times 10^{-4}$ | 0.16 | 0.9999 |
| Cu-8%Cr-1%Al (V2-05-27) | $-9.0 \times 10^{-11}$ | $3.0 \times 10^{-7}$ | $-3.3 \times 10^{-4}$ | 0.16 | 0.9997 |
| Cu-17%Cr-5%Al (as-cast) (8) | $-8.5 \times 10^{-11}$ | $2.8 \times 10^{-7}$ | $-3.2 \times 10^{-4}$ | 0.15 | 0.9998 |
| Cu-23%Cr-5%Al (CS) (heat up) | $-7.6 \times 10^{-11}$ | $2.5 \times 10^{-7}$ | $-3.0 \times 10^{-4}$ | 0.15 | 0.9998 |
| Cu-23%Cr-5%Al (CS) (cool down) | $-5.3 \times 10^{-11}$ | $1.9 \times 10^{-7}$ | $-2.3 \times 10^{-4}$ | 0.13 | 1.0000 |
| NiAl (V2-03-166) | $-7.3 \times 10^{-11}$ | $2.3 \times 10^{-7}$ | $-2.6 \times 10^{-4}$ | 0.12 | 0.9998 |
| Ni-17%Cr-6%Al-0.5%Y (V2-02-27E) | $-9.6 \times 10^{-11}$ | $3.0 \times 10^{-7}$ | $-3.2 \times 10^{-4}$ | 0.15 | 0.9999 |
| Ni-17%Cr-6%Al-0.5%Y (V2-03-528) | $-6.6 \times 10^{-11}$ | $2.4 \times 10^{-7}$ | $-2.8 \times 10^{-4}$ | 0.14 | 1.0000 |

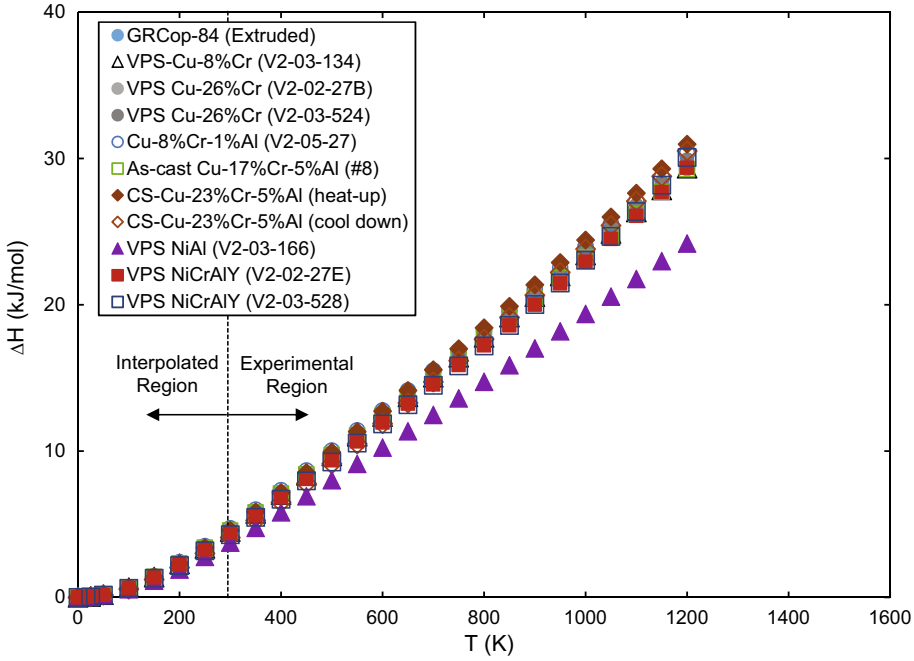


**Fig. 9** Plot of the calculated values of the molar enthalpy against the absolute temperature for variously processed copper alloys, VPS NiAl and VPS NiCrAlY alloys. The calculated values from the experimentally measured $C_P$ data lie to the right of the vertical broken line, while the symbols to the left of this line are based on interpolated values of $C_P$

### 3.4 Comparison with the Dulong–Petit Law

Figure 8 plots the specific molar heat capacity against absolute temperature for the copper alloys, NiAl and NiCrAlY investigated in this study. The atomic weight data used for calculating the molar masses were obtained from Zumdahl (Ref 19). The experimental data lie to right of the vertical broken line at 295 K. The symbols to the left of this line represent the calculated values of $C_P$ determined from empirical polynomial equations fitted to the experimental data. In order to ensure that $C_P = 0$ at $T = 0$ K,[§] the fitting equation used had the form

$$C_P = A_1 * T^4 + B_1 * T^3 + C_1 * T^2 + D_1 * T(\text{J/mol K}) \quad \text{(Eq 5)}$$

where $A_1$, $B_1$, $C_1$ and $D_1$ are regression constants (Table 2). The lower and upper horizontal broken lines represent values of $C_P = 3R$ and $4R$, respectively, where $R$ is the universal gas constant.

The Dulong and Petit law states that $C_V = 3R = 24.9$ J/mol K, where $C_V$ is the specific heat capacity of constant volume, and $R$ is the universal gas constant (Ref 7, 14, 15, 19). Since the molal volume of a solid does not change very much under 1 atm. pressure, $C_P \approx C_V$ (Ref 7, 14, 20, 21). An examination Fig. 8 reveals that except for VPS NiAl, the experimental values of $C_P > 3R$ for all the copper alloys and VPS NiCrAlY. In fact, $C_P \geq 4R$ above 1000 K for Cu-23%Cr-5%Al and NiCrAlY. The fact that $C_P > 3R$ at high temperatures is consistent with reported observations in the

[§]Since the specific heat measurements were not conducted between 0 and 295 K, the form of the Eq 3 has to be consistent with theories on low-temperature specific heat capacities. In the absence of experimental data, Eq 3 is provided to enable the estimation of design parameters of the RLV combustion chamber in the cryogenic range.

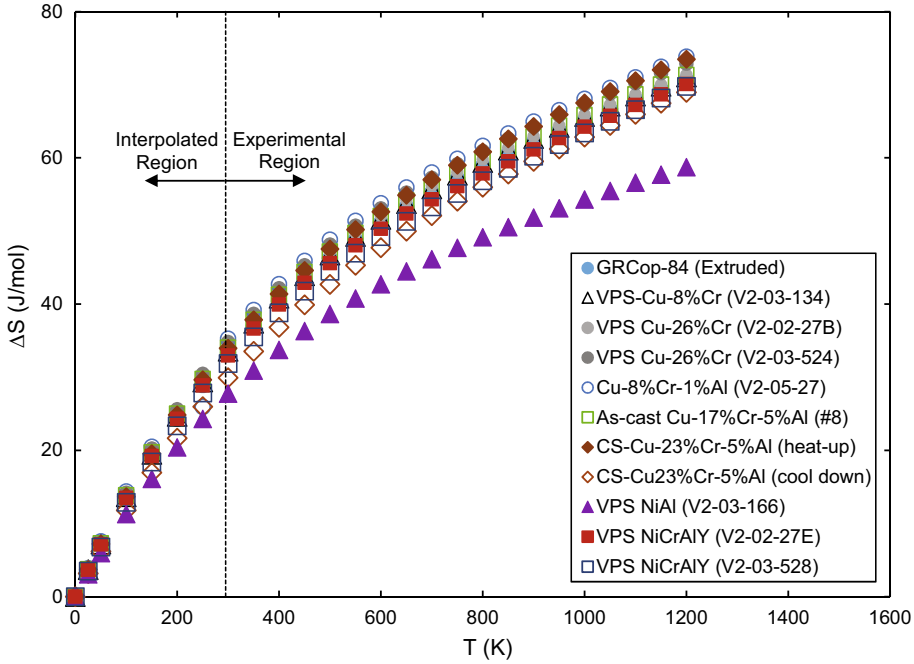


**Fig. 10** Plot of the calculated values of the molar entropy against the absolute temperature for variously processed copper alloys, VPS NiAl and VPS NiCrAlY alloys

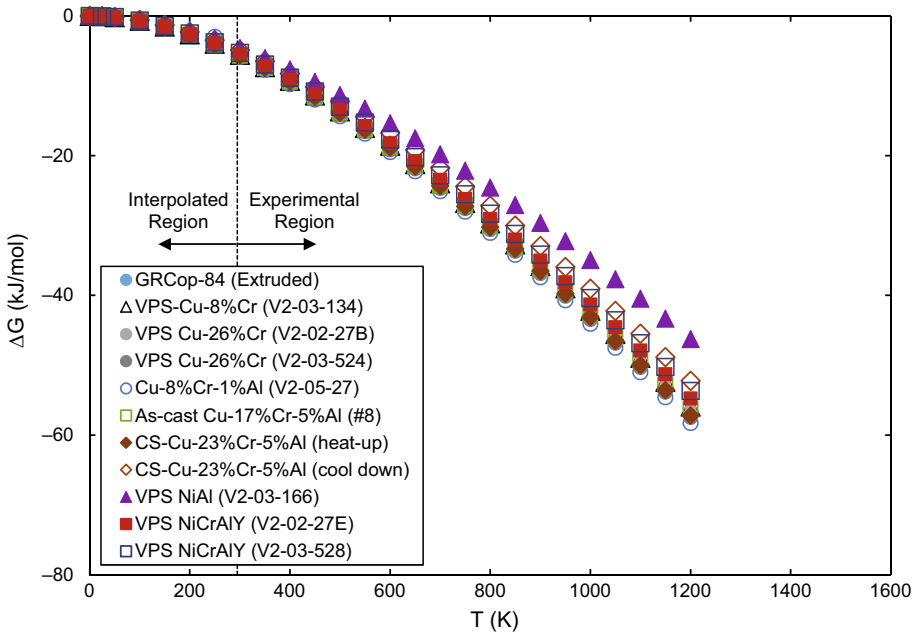


**Fig. 11** Plot of the calculated values of the Gibbs molar free energy against the absolute temperature for variously processed copper alloys, VPS NiAl and VPS NiCrAlY alloys

literature (Ref 7, 14, 21). In the case of VPS NiAl, $C_P < 3R$ at all temperatures but approaches $3R$ above 1100 K.

### 3.5 Evaluation of the Temperature Dependencies of Enthalpy, Entropy and Gibbs Free Energy

The changes in enthalpy, $\Delta H_T$, entropy, $\Delta S_T$, and Gibbs free energy, $\Delta G_T$, were calculated for $0 \leq T \leq 1200$ K using Eq 3, and for simplicity, assuming that the standard reference thermodynamic state is at $T = 0$ K.[§§] The thermodynamic relationships are given by (Ref 7, 14, 21):

[§§]It should be noted that this assumption allows the calculation of the absolute values $H_T$, $S_T$ and $G_T$ rather than $\Delta H_T$, $\Delta S_T$, and $\Delta G_T$.

$$\Delta H_T = H_T = \int_0^T C_P dT \quad \text{(Eq 6)}$$

$$\Delta S_T = S_T = \int_0^T \frac{C_P}{T} dT \quad \text{(Eq 7)}$$

$$\Delta G_T = G_T = \Delta H_T - T * \Delta S_T \quad \text{(Eq 8)}$$

Figures 9, 10 and 11 show the temperature dependencies of $\Delta H_T$, $\Delta S_T$ and $\Delta G_T$ evaluated from Eq 6-8. Once again, the vertical broken lines in the figures denote the experimental and the interpolated regions. The enthalpies for the copper alloys, as well as for VPS NiCrAlY, are extremely close and indistinguishable in Fig. 9 between 0 and 1223 K. At 1200 K, the lowest value of $\Delta H_T \approx 29.3$ kJ/mol in this band is for VPS Cu-26%Cr and the highest value of $\Delta H_T \approx 31.0$ kJ/mol is for CS Cu-23%Cr-5%Al. The enthalpy curve for VPS NiAl falls below those for the copper alloys and VPS NiCrAlY and increasingly deviates away from the other curves with increasing absolute temperature (Fig. 9). At 1200 K, the magnitude of $\Delta H_T \approx$ 24.2 kJ/mol for NiAl. The enthalpy increases with absolute temperature for all the materials.

The molar entropy increases at a decreasing rate with increasing absolute temperature for all the alloys studied in the present investigation (Fig. 10). The values of $\Delta S_T$ for the copper alloys and VPS NiCrAlY fall within a relatively narrow band with a maximum spread of about 4.5 J/mol. The maximum and minimum values of 73.8 and 69.0 J/mol occur at 1200 K for VPS Cu-8%Cr-1%Al and CS Cu-23%Cr-5%Al (cool down), respectively. The average maximum value of $\Delta S_T$ for the other alloys at 1200 K is 71.3 J/mol. The data for $\Delta S_T$ for VPS NiAl are well below this band with the maximum value of about 58.7 J/mol occurring at 1200 K.

The Gibbs free energy decreases with increasing absolute temperature (Fig. 11). The lowest value of $\Delta G_T$ at 1200 K is for VPS Cu-8%Cr-1%Al, which was estimated to be about − 58.3 kJ/mol. The highest magnitude of $\Delta G_T$ at 1200 K was for VPS NiAl with an estimated value of about − 46.3 kJ/mol.

## 4. Summary and Conclusion

The temperature dependencies of the constant-pressure specific heat capacities, $C_P$, of several vacuum plasma-sprayed (VPS) and cold-sprayed copper alloy monolithic coatings, VPS NiAl, VPS NiCrAlY, extruded GRCop-84 and as-cast Cu-17(wt.%)Cr-5%Al are discussed. The magnitudes of $C_P$ increased with increasing temperature for all the alloys with the data falling within a narrow scatter band for most of the Cu-Cr alloys but well separated for the NiAl and NiCrAlY coatings. The data were well represented by empirical polynomial equations, and the evaluated values of the regression coefficients are reported. The experimental data did not agree with values calculated from the empirical Neumann–Kopp rule. Instead, a modification of the Neumann–Kopp rule was found to predict values closer to the experimental data with an absolute deviation less than 6.5%. The molar specific heat capacities for the alloys did not agree with the Dulong–Petit law. Instead, the magnitudes of $C_P > 3R$, where $R$ is the universal gas constant, at all temperatures for all the alloys except VPS NiAl for which $C_P < 3R$. The values of molar enthalpy, molar entropy and Gibbs molar free energy calculated from the molar specific heat capacities are reported for the investigated alloys.

## Acknowledgments

The experimental measurements were conducted by the Thermophysical Properties Research Laboratory, Inc. (TPRL), West Lafayette, IN under contract, and these contributions are gratefully acknowledged.

## References

1. S.V. Raj, Thermophysical Properties of Cold- and Vacuum Plasma-Sprayed Cu-Cr-X Alloys, NiAl and NiCrAlY Coatings I: Electrical and Thermal Conductivity, Thermal Diffusivity, and Total Hemispherical Emissivity, *J. Mater. Eng. Perform.*, 2017. doi:10.1007/s11665-017-3012-0
2. S.V. Raj and A. Palczer, Thermal Expansion of Vacuum Plasma Sprayed Coatings, *Mater. Sci. Eng. A*, 2010, **A527**, p 2129–2135
3. S.V. Raj, R. Pawlik, and W. Loewenthal, Young's Moduli of Cold and Vacuum Plasma Sprayed Metallic Coatings, *Mater. Sci. Eng. A*, 2009, **A513-514**, p 59–63
4. J. Karthikeyan, *Development of Oxidation Resistant Coatings on GRCop-84 Substrates by Cold Spray Process, NASA CR 2007–214706*, NASA Glenn Research Center, Cleveland, 2007
5. http://www.tprl.com/tprl.html
6. ASTM Standard E1269, Standard test method for determining specific heat capacity by differential scanning calorimetry, *ASTM Annual Book of Standards,* vol. 14.02 (ASTM International, West Conshohocken, 2004)
7. G.N. Lewis and M. Randall, *Thermodynamics*, 2nd ed., McGraw-Hill, New York, 1961, p 66
8. D.O. Allison, *Polynomial Approximations of Thermodynamic Properties of Arbitrary Gas Mixtures Over Wide Pressure and Density Ranges, NASA TN D-6862*, National Aeronautics and Space Administration, Washington, 1972
9. J.R. Andrews and O. Biblarz, *Temperature Dependence of Gas Properties in Polynomial Form, NPS67-81-001*, Naval Postgraduate School, Monterey, 1981
10. B.J. McBride, S. Gordon, and M.A. Reno, *Coefficients for Calculating Thermodynamic and Transportation Properties of Species, NASA TM 4513*, National Aeronautics and Space Administration, Washington, 1993
11. R. Hickman, T. McKechnie, and R. Holmes, Material Properties of Vacuum Plasma Sprayed Cu-8Cr-4Nb for Liquid Rockets, *37th Joint Propulsion Conf.*, Salt Lake City, UT, 2001, American Institute for Aeronautics and Astronautics, Washington, DC
12. Y.S. Touloukian and E.H. Buyco, *Specific Heat: Metallic Elements and Alloys, Thermophysical Properties of Matter*, Vol 4, IFI/Plenum, New York, 1970, p 146–152
13. W.S. Walston and R. Darolia, Effect of Alloying on Physical Properties of NiAl, *High-Temperature Ordered Intermetallic Alloys V*, (eds. I. Baker, R. Darolia, J.D. Whittenberger, and M.H. Yoo, 1993, vol. 288, p. 237–242, *MRS Symposium Proceedings*, Materials Research Society, Pittsburgh, PA
14. L.S. Darken and R.W. Gurry, *Physical Chemistry of Metals*, McGraw-Hill, New York, 1953
15. R.A. Swalin, *Thermodynamics of Solids*, Wiley, New York, 1962
16. J. Valencia and P.N. Quested, Thermophysical Properties, *ASM Handbook*, 2008, **15**, p 468–481
17. J. Leitner, P. Vonka, D. Sedmidubsky, and P. Svoboda, Application of Neumann–Kopp Rule for the Estimation of Heat Capacity of Mixed Oxides, *Thermochim. Acta*, 2010, **497**, p 1–13
18. R. Brandt, L. Pawlowski, G. Neuer, and P. Fauchais, Specific Heat and Thermal Conductivity of Plasma Sprayed Yttria-Stabilized Zirconia and NiAl, NiCr, NiCrAl, NiCrAlY, NiCoCrAlY Coatings, *High Temp. High Press.*, 1986, **18**, p 65–77
19. S.S. Zumdahl, *Introductory Chemistry*, 5th ed., Houghton Mifflin Co., Boston, 2004
20. N.F. Mott and H. Jones, *The Theory of the Properties of Metals and Alloys*, Dover, New York, 1958
21. H. Wang, R. Lück, and B. Predel, Heat Capacities of Intermetallic Compounds in the Iron-Titanium System, *Z. Metall.*, 1993, **84**, p 230–236